

# ILLUMINANCE-PROXY HIGH DYNAMIC RANGE IMAGING: A SIMPLE METHOD TO MEASURE SURFACE REFLECTANCE

**Mardaljevic, J.**<sup>1</sup> and Brembilla, E., and Drosou, N.  
School of Civil and Building Engineering, Loughborough University,  
Loughborough, Leicestershire, LE11 3TU, UK  
<sup>1</sup>j.mardaljevic@lboro.ac.uk

## Abstract

A technique to measure arbitrarily complex patterns of diffuse surface reflectance under real-world illumination conditions is presented. The technique is founded on high dynamic range (HDR) imaging whereby the luminance values in an HDR image are used to derive average and/or per-pixel values of surface reflectance. Two variants of the method are described and the results from both are compared with analytical solutions. Whilst the technique has general application for the measurement of reflectance, the authors make the case that there is a pressing need to survey occupied building spaces since the notional/typical reflectance values commonly employed in simulation for compliance testing may be quite different from those found in real buildings.

*Keywords:* Reflectance, High Dynamic Range Imaging, Illuminance Measurement.

## 1 Introduction

The accurate representation of surface reflectance values is an essential component of any lighting evaluation method, be it analytical, physical (e.g. scale model) or simulation based. For scale models the finish can usually be used directly in the model construction, unless it has a large scale pattern-repeat, or if it is some unique or difficult to reproduce material, e.g. a silk wall hanging in a heritage building.

The area-weighted mean reflectance  $\bar{\rho}_w$  of any surface composed of a 'patchwork' of  $n$  areas of different diffuse reflectivity is the sum of the product of area  $\times$  reflectivity for each individual patch, divided by the total area  $A$  of all the individual patches:

$$\bar{\rho}_w = \frac{a_1\rho_1 + a_2\rho_2 + \dots + a_n\rho_n}{a_1 + a_2 + \dots + a_n} = \frac{\sum_{i=1}^n a_i\rho_i}{A} \quad (1)$$

The area-weighted mean reflectance (AWMR) is commonly employed to calculate the average daylight factor using the revised equation devised by Crisp and Littlefair (Crisp et al., 1984). For this application the reflectances of the primary surfaces, e.g. the floor, walls, ceiling, etc. are usually taken from manufacturers' data or estimated from charts. However, diffuse reflectance  $\rho$  may be derived directly from samples of, say, paint finish using combined measurements of luminance  $L$  and illuminance  $E$  and applying the relation:

$$\rho = \frac{\pi L}{E} \quad (2)$$

Alternatively, reflectance can also be derived from relative measurements of luminance between the sample and one or more standard diffuse reflectors under the same lighting conditions.

The basic technique becomes onerous or even impractical when the number of individual surfaces, each with their own unique reflectance, becomes large. Additionally there is the problem of reliably measuring the area of each patch. For patterned wallpapers and similar finishes, it is often a matter of judgement rather than direct measurement to assign a representative reflectance value to the overall finish.

### 1.1 Surface reflectance and design compliance

In 2013 the UK Education Funding Agency (EFA) made climate-based daylight modelling (CBDM) a mandatory requirement for the evaluation of designs submitted for the Priority Schools Building

Programme (PSBP) (Education Funding Agency, 2014). School designs submitted to the PSBP must achieve certain ‘target’ criteria for the useful daylight illuminance (UDI) metric. This is believed to be the first major upgrade to mandatory daylight requirements since the introduction of the daylight factor more than half a century ago. In the US, a climate-based daylight metric approved by the IESNA has appeared in the latest version of LEED (Illuminating Engineering Society, 2012).

The PSBP daylight criteria were formulated by consulting engineers working in conjunction with the EFA (Mardaljevic, 2015). They decided to base the criteria on UDI. The UDI scheme is founded on occupant responses to daylight levels, as reported in several studies – see the original UDI papers for these (Nabil et al., 2005)(Nabil et al., 2006). The PSBP requirement specifies that the space-averaged value for the occurrence of illuminances in the range 100 to 3,000 lux during the period 08h30 to 16h00 is 80%.

Relatively small changes in prescribed or assumed surface reflectance values can determine whether a design passes or fails the compliance target. The examples shown in Figure 1 give the UDI predictions for the same classroom design with different reflectivity values for the wall and ceiling. In one the ceiling and wall reflectance values were 0.80 and 0.60 (respectively), in the other they were 0.70 and 0.50 (values typically recommended in guidelines). The classroom with the lower reflectance values just fails to achieve the target of 80% space-averaged UDI and would be deemed not to have ‘passed’. The plots in Figure 1 also show the occurrence for the ranges 100 to 300 lux and 300 to 3,000 lux.

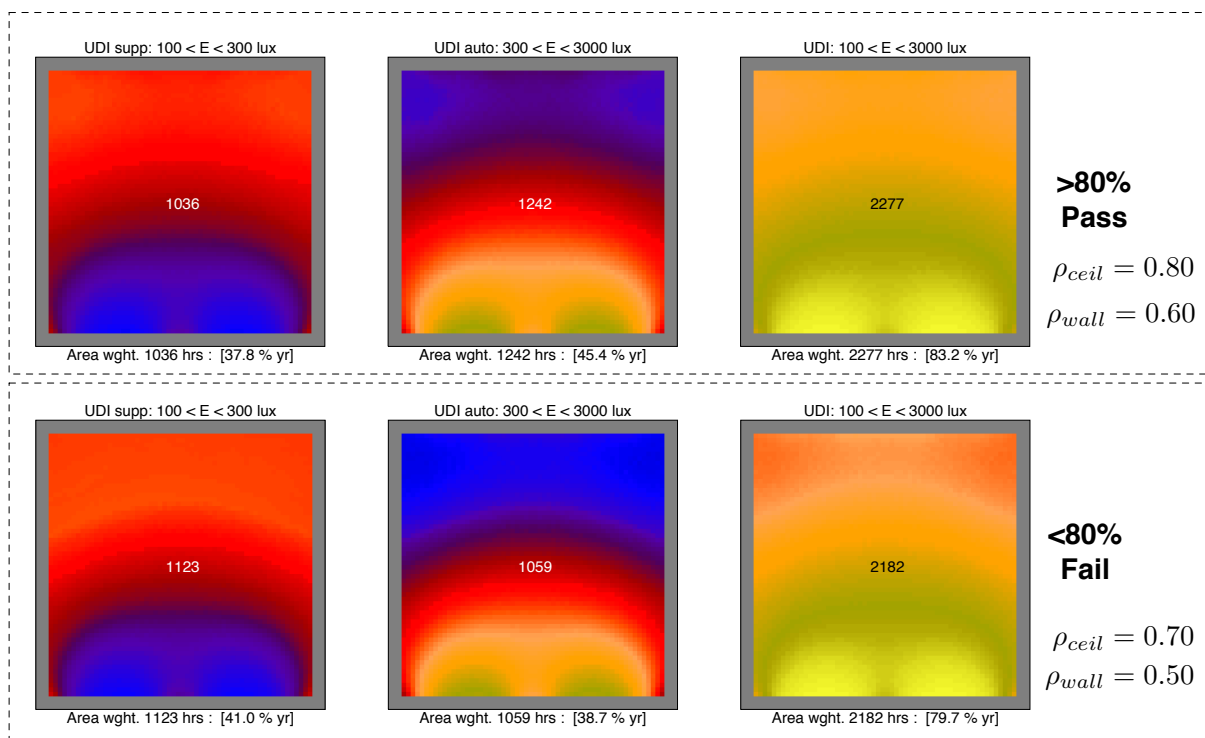


Figure 1 – Pass/fail UDI examples

## 2 Measuring illuminance with high dynamic range imaging

### 2.1 Background

A recent technology called high dynamic range (HDR) imaging has greatly expanded our capacity to measure luminous quantities. A high dynamic range (HDR) image is one where every pixel contains a luminance reading for that point in the recorded scene, in other words: a measurement of luminance. There are a small number of specialist HDR cameras on the market, however it is possible to create HDR images from multiple exposures taken by consumer digital cameras which can have up to 10 million or more pixels (Reinhard et al., 2005). A consumer digital camera is

used to capture a controlled sequence of exposures covering a wide range of exposure values, e.g. from 1/1000 s to 1 s at a fixed aperture. The images are 'compiled' into a single HDR image where each pixel now contains a derived measure of the luminance (in  $\text{cd/m}^2$ ) of that point in the scene. With suitable calibration using a single spot measurement taken with a traditional photometer, the absolute accuracy of the luminance values in the HDR image is typically better than  $\pm 20\%$  and often as good as  $\pm 10\%$ .

Use of HDR as a proxy for illuminance has been demonstrated by a number of authors (Mardaljevic et al., 2009)(Bellia et al., 2011). In the approach described by Mardaljevic et al., the luminance 'seen' (by the HDR camera) on one side of a diffusely transmitting material resulting from incident illuminance on the other side is used to derive the magnitude and the distribution of the incident illuminance field. The examples given include the measurement of the lumen output of daylight window and a light pipe. Bellia et al. use the relation given in equation 2 to directly determine the illuminance incident on 'target' cards of known reflectance distributed on the desks of classrooms. In effect, each card in the HDR image acts as an illuminance meter.

Image-based determination of the reflection (or albedo) map of a surface is an established technique that has its origin in remote sensing. Map here is used to refer to a pixel-by-pixel evaluation of albedo / reflectivity. Innovative techniques have been applied to extract depth information as well as reflectivity from digital images (Glencross et al., 2008). Put simply, if an image contains a reliable measure of luminance  $L$  on a per-pixel basis, the the reflectivity on a per-pixel basis can be determined using equation 2 provided that the incident illuminance  $E$  on a per-pixel basis is also known.

Techniques developed for computer graphic applications tend to focus on the accurate representation of 'textures' in computer generated images, in particular, irregular surface finishes that do not lend themselves to representation by formula-based descriptions, e.g. stone, sand, etc. Paired photos taken with and without a controlled flash exposure is one of the methods used to determine the albedo maps. In this approach, a calibration image of a diffusely reflecting white surface is taken using a controlled flash exposure at a set distance from the surface. Then, from the same distance, the test sample, say, an area of stone surface, is photographed twice: once under ambient light conditions and then with the controlled flash exposure. From these two images it is possible to infer the incident illumination field (Glencross et al., 2008). This approach neatly incorporates the effect of vignetting and other angle dependant factors.

Somewhat overlooked in the discipline of computer graphics is the arguably more straightforward matter of measuring bulk surface reflectance properties for the purpose of incorporating them into lighting simulation to predict illuminance quantities rather than images. Daylight evaluations at the design stage typically involve simulation to demonstrate that the illumination in the proposed building meets various daylight criteria. As noted, until recently those criteria were based almost without exception on the daylight factor. Whatever the method, daylight factor or CDBM, the outcome can depend strongly on the reflectance properties assigned to the key surfaces, e.g. ceiling, walls, and (to a lesser degree) the floor.

Simulation models are invariably 'empty box' representations of real spaces. Walls, ceiling and the floor are usually given reflectance values based on paint and material samples. Surfaces are represented in the simulation without any form of 'clutter'. Whilst the introduction of arbitrary factors must be avoided in any compliance procedure, the following question needs be asked: how do real spaces compare to simulated ones with respect to daylighting performance? In order to answer this, a method for surveying real spaces is needed that is neither too onerous nor too complex. A simple method that fits these requirements is described below.

## 2.2 Overview of the illuminance proxy HDR method

The proposed method is in fact a modest, apparently overlooked, refinement of the existing illuminance proxy techniques noted above. Two variants of the proposed technique are described: a basic method which can be carried out using readily available tools, and a refined method which may require bespoke programming to carry out some fairly standard image processing routines (e.g. interpolation). The basic method is founded on the premise that the area-weighted diffuse reflectance of a surface can be determined from an HDR image providing that:

- The images are taken normal to the surface in question.

- The surface finish does not contain any significant specular component.
- The illumination field across the surface does not contain very steep gradients or step changes.
- Vignetting correction is either not needed or known and can be applied.
- No other significant lens distortions (e.g. pin-cushion or barrel) are present.

In addition to the above, the refined method also delivers a pixel-by-pixel reflectance map of the surface. The two approaches are demonstrated below through application to test surfaces containing patches of known reflectivity where an analytical evaluation of the area-weighted mean reflectance can be made. Put simply, data from the HDR image are used to solve for the reflectivity  $\rho$  in equation 2.

### 2.3 The test surfaces

Two test surfaces comprising PDF images of shaded circles printed on to white and black backgrounds were used to test the HDR derived measurements of area-weighted mean reflectance. The images were composed using a drawing tool and printed onto normal A3 paper using a typical photocopier/printing machine. The two images comprise identical arrangements of circles of various sizes against a white or black background, Figure 2. The 'target area' has dimensions  $36 \times 24$  cm and its extent is delineated by the dashed lines in the greyscale images and the right-angle corner markers in the falsecoloured HDR images. Just one shade of black and one of grey were used – otherwise, the white is the base colour of the paper. The reflectivity of the black, grey and white areas were calculated from simultaneous measurements of illuminance and luminance using, respectively, a Hagner EC1-X meter and a Konica-Minolta LS100 spot photometer. Multiple measurements under daylight conditions were taken, and the reflectivity determined from the average of the values calculated using equation 2. Based on the mean of multiple measurements, the reflectivities for the black, grey and white surfaces were 0.04, 0.26 and 0.77, respectively. Note, some care must be taken to minimise the specular component of reflections when taking measurements since photocopier toner can be noticeably 'shiny'.

Employing these measured values, the area-weighted mean reflectance for each printed image was predicted using Equation 1. The calculated area-weighted mean reflectance values were: 0.484 (black/grey circles on a white background) and 0.296 (white/grey circles on a black background).

### 2.4 Basic method: illuminance values estimated from point samples

HDR image captures of the printed images were then taken under stable daylight conditions and displayed/analysed using the freely-available HDR image browser Photosphere.<sup>1</sup> A false-colour HDR luminance image is shown below the respective black/grey/white images in Figure 2. For the basic method, the AWMR is estimated from the HDR assuming a single incident illuminance value  $\bar{E}$  which is based on the mean of 10 'spot' luminance values of the white area distributed across the image, i.e. the red crosses in Figure 2. The illumination across the A3 printed images shown in Figure 2 was very even – a claim easily verified from the narrow range in the 10 'spot' luminance values taken from the HDR captures. For the white background image the range varied between  $25.9 \text{ cd/m}^2$  and  $28.7 \text{ cd/m}^2$ , whereas for the black background image the range was  $24.5 \text{ cd/m}^2$  to  $25.7 \text{ cd/m}^2$ .

Taking the mean in each case and applying Equation 2, the estimated mean illuminance across the two images at the time of HDR capture was 111 lx and 102 lx for the white and black background, respectively. Next, the mean luminance  $\bar{L}_{hdr}$  of all the pixels in the rectangular area of the HDR image that correspond to the  $36 \times 24$  cm 'target area' was determined using the selection tool in Photosphere. Those values were  $17.5 \text{ cd/m}^2$  and  $10.1 \text{ cd/m}^2$ . Then, applying again Equation 2, the area-weighted mean reflectance values determined from the HDR images ( $\bar{\rho}_{hdr}$ ) were 0.497 and 0.312. These HDR derived AWMR values are in good agreement with those based on direct measurements. The various calculated, measured and derived quantities used for this simplified approach are given in Table 1.

<sup>1</sup> Available from Greg Ward's website: <http://www.anyhere.com>

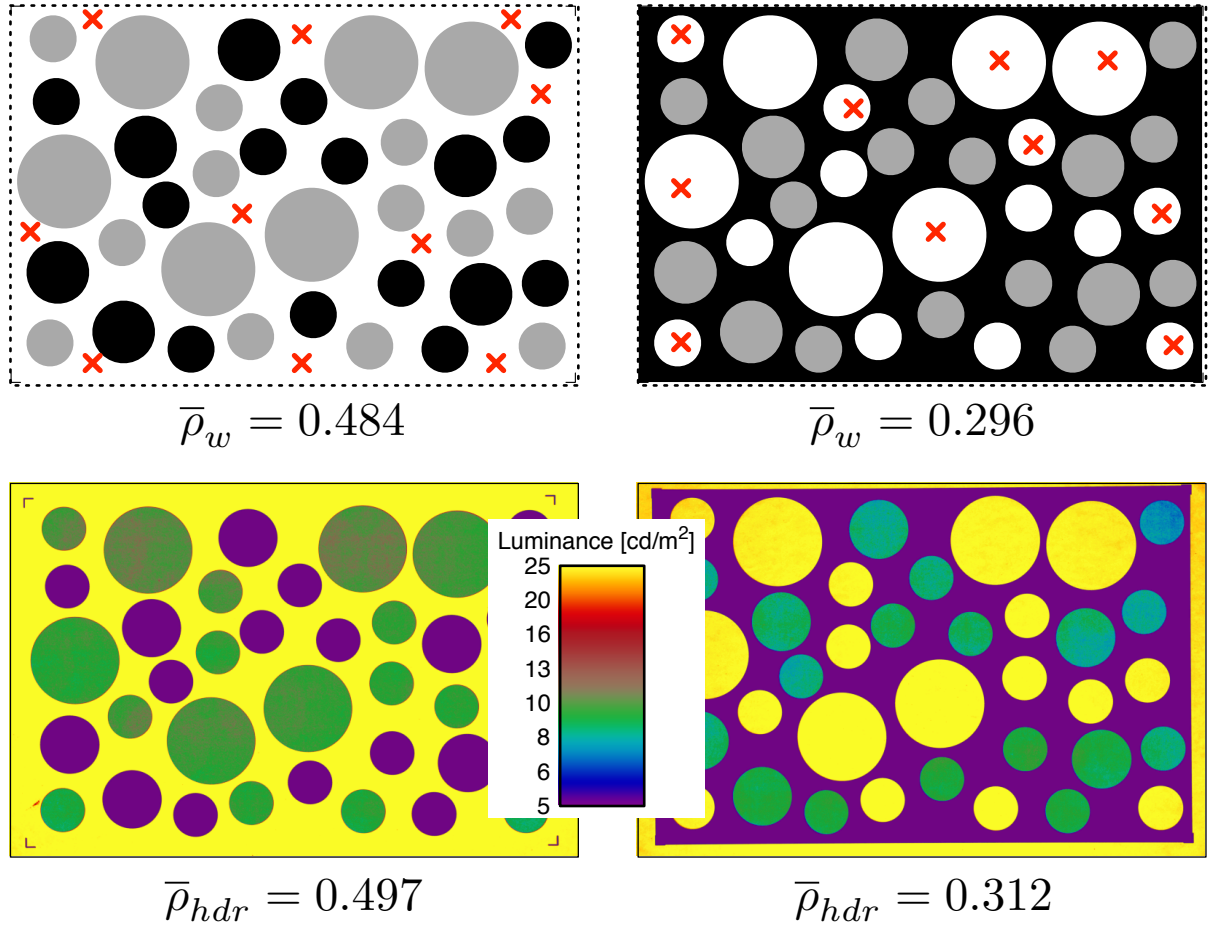


Figure 2 – Test surfaces and HDR captures

### 2.5 Refined method: pixel illuminance values determined from gridding

For the refined method, the illuminance field  $\mathbf{E}_{hdr}$  across the HDR image  $\mathbf{L}_{hdr}$  is determined on a pixel basis using surface interpolation, a technique also referred to as gridding. The gridding function interpolates a limited number of illuminance values at various irregularly located points on the test images to create a regular grid which is defined by the pixel dimensions of the HDR image, i.e. there is a one-to-one correspondence between pixels in the interpolated image and the HDR image.

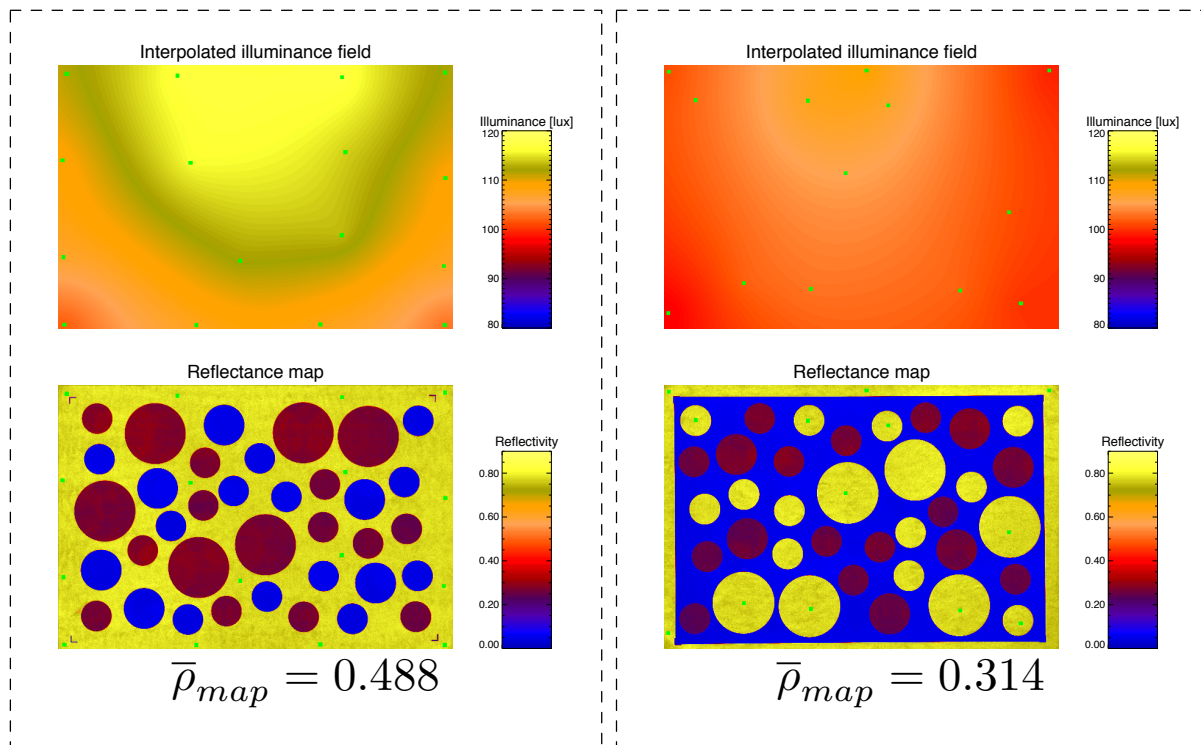
Equation 2 is now applied using the interpolated illuminance field  $\mathbf{E}_{hdr}$  and the HDR luminance image  $\mathbf{L}_{hdr}$ , resulting in a reflectance map  $\rho_{map}$  for the image. That is, an array with the same dimensions as the original HDR image and containing the pixel-by-pixel reflectance values for the surfaces in the image. The interpolated illuminance fields and the derived reflectance maps for the two test surfaces are given in Figure 3. For both images the interpolated illuminance field showed the highest values at the middle of the upper part of the image, i.e. the illumination was from above. The small green squares indicate the scattered data points which were the basis for the interpolated grid. These were all on the white areas of the paper since, as previously, white paper serves as the ‘reference’ reflectivity (i.e.  $\rho = 0.77$ ).

The target area of the image comprised approximately 15 million pixels. The mean of the target area pixels in the reflectance maps for the two surfaces was 0.488 and 0.314 for the white and black background images, respectively. These values compare very well with the analytically derived values and those from the simplified HDR method. The good agreement between the mean reflectance determined using the simple and gridded methods is perhaps not surprising since the variation in the illuminance field across the target areas was small. Thus the mean value estimate from the simple method agreed closely with the mean of the target area pixels for

**Table 1 – Basic method using illuminance values estimated from point samples**

Quantity	White background	Black background
Calculated AWMR	0.484	0.296
Mean of 10 luminance values (white)	27.13 cd/m <sup>2</sup>	24.95 cd/m <sup>2</sup>
Mean illuminance across image	111 lx	102 lx
Mean luminance of HDR pixels	17.5 cd/m <sup>2</sup>	10.1 cd/m <sup>2</sup>
HDR derived AWMR - simple	0.497	0.312
Percentage divergence in AWMR	2.7%	5.4%
HDR derived AWMR - grid	0.488	0.314
Percentage divergence in AWMR	0.8%	6.1%

the interpolated grid.

**Figure 3 – Interpolated illuminance fields and derived reflectance maps**

## 2.6 Example application

The example used to demonstrate practical application is a section of wall in a side-lit stairwell. The target area comprises a mixture of roughly finished concrete and dark brick with a wooden handrail, Figure 4. Seven white cards of known reflectance were placed around the target area delineated by the green box. An HDR image was taken under steady illumination conditions. Using the procedures for the refined method, the illuminance field was interpolated using the registration points on the white cards (marked as green squares in the plots). Where it is evident that the illumination field is varying significantly over the area of one of the cards, it may be worthwhile to select more than one registration point on that card to help the gridding routine resolve the gradients.

The interpolated illumination field varied between  $\sim 200$  to  $\sim 800$  lx, with a fairly steep gradient around the white card closest to the windows (Figure 4). The estimation perhaps would have benefitted from a greater number of white cards encircling the target area. The mean reflectivity across the target area was determined to be 0.159, or approximately 16%.



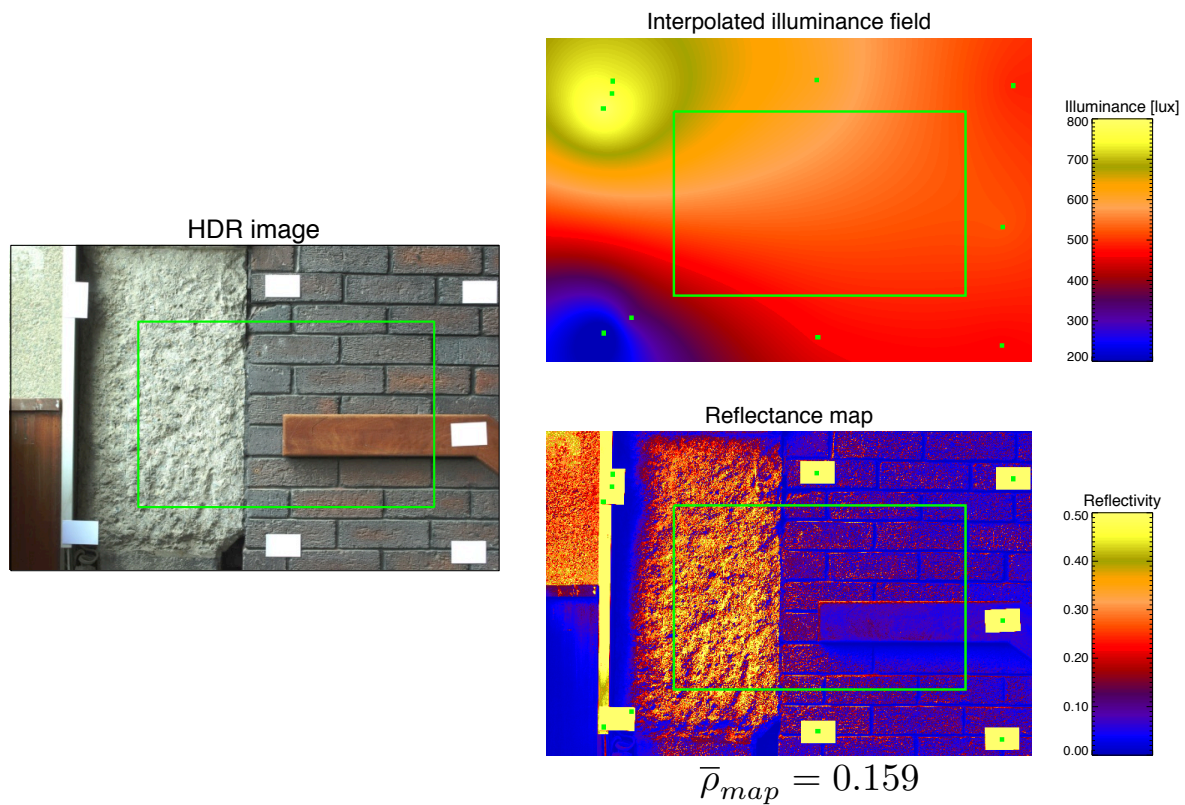


**Figure 4 – Mean reflectance for boxed area determined from an HDR image and interpolated illuminance field**

### 3 Discussion

This paper has described the application of a simple technique to measure mean surface reflectance and/or derive a reflectance map using HDR imaging. The approach is ideally suited for the surveying of, say, wall reflectance values in real spaces with the minimum of effort. The initial results are promising, though further testing validation testing is advised. Vignetting was not an issue for the cases described here, however surveying of real spaces would probably require the use of wide-angle lenses – the HDR images taken with these will require correction to address the fall-off in luminance towards the periphery of the image field (Jacobs et al., 2007).

The area of wall used for the example application included surfaces that were ‘textured’ in various ways, e.g. roughly finished concrete, bricks and the handrail (Figure 4). For any surface with texture the condition of diffuse reflectivity no longer strictly applies because the luminance of the surface at any point will depend on the direction of the incoming illumination as well as the magnitude (Ward, 1992). So, equation 2 no longer strictly applies. However, the degree to which it no longer applies depends entirely on the specifics, e.g. type of surface articulations, surface reflectivity, incident illumination field, etc. And, of course, the significance of any divergence between ideal and actual behaviour of a reflecting surface may not be great in any practical application, e.g. the simulation of illumination in a space.

Lighting simulation for compliance purposes is invariably carried out using ‘empty’ building models which contain the bare minimum of geometrical details. Thus, whilst facade elements such as glazing and window reveals are often modelled in detail, the rest of the internal enclosure for a (rectangular) space is often little more than five planar surfaces: side and back walls, floor and ceiling. If not specified, these surfaces are typically assigned default reflectivity values of, say: 20%, 50% and 70% for the floor, walls and ceiling, respectively.

However, any real space once furnished and occupied will differ greatly in appearance to the

simulated space, Figure 5. A question presents itself: does it matter if the surfaces properties in an actual space differ greatly from what was simulated? Increasingly, a consensus seems to be developing amongst building scientists that predicted energy performance should strive to match actual building performance (Lewry, 2015). For daylight illumination in buildings the situation is very different since illumination or indeed any illumination-related quantity is very rarely measured in buildings, and then not as a matter of routine and logged with the more usual parameters (room temperature, CO<sub>2</sub> levels, etc.) by the building energy management system. Consequently, validation of daylighting performance becomes highly problematic. Even testing for compliance with daylight factor predictions is rather less straightforward than many imagine since the occurrence of overcast skies that conform well to the CIE standard overcast luminance pattern is both rare and difficult to identify (Mardaljevic, 2004). For climate-based predictions any validation would be even more challenging since absolute measures of illuminance would need to be measured over long time periods (Mardaljevic, 2015).



**Figure 5 – Real and simulated classroom (different designs)**

The situation is not however as gloomy as it might appear from the above. The underlying simulation engine for CBDM has undergone rigorous valuation and proven to be capable of very high accuracy (Mardaljevic, 2000) (Mardaljevic, 2001). As noted, energy performance of the completed building often differs markedly from what was simulated. Energy consumption of a building depends on numerous factors – not just the thermo-physical properties of the building, but also the operational and behavioural characteristics. Although CBDM arrived two or more decades after dynamic thermal modelling became established, a reliable prediction of the daylighting performance of the *fixed* architectural form of the building should in fact be easier to achieve than a reliable prediction of, say, the energy consumption. For the simple reason that, unlike the thermo-physical response of a building, the (instantaneous) daylight conditions depend only on the state of the building (and the sun and sky conditions) at that moment – there is no illumination equivalent of thermal lag/inertia. Consequently, performance dependencies with (fixed building form) daylight are far less complex, with few if any 'knock-on' effects. Recently begun studies comparing UDI predictions using totally different CBDM formulations have shown good similarity in output so far (Brembilla et al., 2015a) (Brembilla et al., 2015b).

It is proposed that the techniques described here to measure surface reflectance should be used to survey real spaces. Then, the discrepancy between actual reflectance values and those notional/typical values commonly employed for compliance purposes should be evaluated in terms of their effect, if any, on predicted outcomes using simulation, i.e. pass or fail for various compliance targets. At the time of writing, the authors are engaged in expanding on the work described here with an emphasis on classrooms and school design where, in the UK, there is particular interest because of the mandatory evaluation requirements founded on climate-based daylight modelling (Drosou, 2015).



## Acknowledgements

Prof. Mardaljevic acknowledges the support of Loughborough University. Ms. Brembilla acknowledges the support of EPSRC and industrial partner Arup, and Ms. Drosou the support of the EPSRC LoLo Doctoral Training Centre in Energy Demand.

## References

- BELLIA, L., MUSTO, M. and SPADA, G., 2011. Illuminance measurements through hdr imaging photometry in scholastic environment. *Energy and Buildings*, 43(10), 2843–2849.
- BREMBILLA, E., MARDALJEVIC, J. and ANSELMO, F., 2015a. The effect of the analysis grid settings on daylight simulations with Climate-Based Daylight Modelling. In *28th CIE Session*, Manchester.
- BREMBILLA, E., MARDALJEVIC, J. and HOPFE, C. J., 2015b. Sensitivity Analysis studying the impact of reflectance values assigned in Climate-Based Daylight Modelling. In *Building Simulation Conference*, Hyderabad.
- CRISP, V. H. C. and LITTLEFAIR, P. J., 1984. Average daylight factor prediction. *Proc. Nat. Lighting Conf., Cambridge (London: CIBSE)*.
- DROU, N., 2015. Uncharted territory - daylight performance and occupant behaviour in a live classroom environment. *6th VELUX Daylight Symposium, London, UK. 2-3 September*.
- EDUCATION FUNDING AGENCY, 2014. EFA daylight design guide - version 2. *Department For Education, UK*.
- GLENCROSS, M., WARD, G. J., MELENDEZ, F., JAY, C., LIU, J. and HUBBOLD, R., 2008. A perceptually validated model for surface depth hallucination. In *ACM SIGGRAPH 2008 Papers*, SIGGRAPH '08, New York, NY, USA: ACM, pp. 59:1–59:8.
- ILLUMINATING ENGINEERING SOCIETY, 2012. Approved Method: IES Spatial Daylight Autonomy (sDA) and Annual Sunlight Exposure (ASE). *IES LM-83-12*.
- JACOBS, A. and WILSON, M., 2007. Determining lens vignetting with HDR techniques. *Bulgarian National Lighting Conference, 10–12 June, Varna, Bulgaria*.
- LEWRY, A., 2015. Bridging the performance gap: Understanding predicted and actual energy use of buildings. *Building Research Establishment, Garston, UK*, IP 1/15.
- MARDALJEVIC, J., 2000. *Daylight Simulation: Validation, Sky Models and Daylight Coefficients*. Ph.D. thesis, De Montfort University, Leicester, UK.
- MARDALJEVIC, J., 2001. The BRE-IDMP dataset: a new benchmark for the validation of illuminance prediction techniques. *Lighting Research and Technology*, 33(2), 117–134.
- MARDALJEVIC, J., 2004. Verification of program accuracy for illuminance modelling: Assumptions, methodology and an examination of conflicting findings. *Lighting Research and Technology*, 36(3), 217–239.
- MARDALJEVIC, J., 2015. Climate-Based Daylight Modelling And Its Discontents. *CIBSE Technical Symposium, London, UK*, 16-17 April.
- MARDALJEVIC, J., PAINTER, B. and ANDERSEN, M., 2009. Transmission illuminance proxy HDR imaging: A new technique to quantify luminous flux. *Lighting Research and Technology*, 41(1), 27–49.
- NABIL, A. and MARDALJEVIC, J., 2005. Useful daylight illuminance: a new paradigm for assessing daylight in buildings. *Lighting Research and Technology*, 37(1), 41–57.
- NABIL, A. and MARDALJEVIC, J., 2006. Useful daylight illuminances: A replacement for daylight factors. *Energy and Buildings*, 38(7), 905–913.

REINHARD, E., WARD, G., PATTANAİK, S. and DEBEVEC, P., 2005. *High Dynamic Range Imaging: Acquisition, Display, and Image-Based Lighting (The Morgan Kaufmann Series in Computer Graphics)*. San Francisco, CA, USA: Morgan Kaufmann Publishers Inc.

WARD, G. J., 1992. Measuring and modeling anisotropic reflection. In *SIGGRAPH '92: Proceedings of the 19th annual conference on Computer graphics and interactive techniques*, New York, NY, USA: ACM Press, pp. 265–272.